Available online at www.sciencedirect.com
SCIENCE DIRECT®
PERGAMON
Deep-Sea Research I 50 (2003) 701–719
DEEP-SEA RESEARCH PART I
www.elsevier.com/locate/dsr

Spreading of Labrador sea water: an advective-diffusive study based on Lagrangian data ☆

Fiammetta Straneo*, Robert S. Pickart, Kara Lavender

Department of Physical Oceanography, Woods Hole Oceanographic Institution, Clark 354A MS 21, Woods Hole, MA 02543, USA

Received 1 March 2002; received in revised form 18 September 2002; accepted 5 March 2003

Abstract

The pathways and timescales for the spreading of Labrador Sea Water (LSW) in the subpolar North Atlantic are investigated with an advective–diffusive model. The model's mean flow and eddy diffusivity are derived from float measurements, while the region of LSW formation is obtained from hydrographic data. Two main export pathways for LSW are reproduced by the model: eastward into the Irminger Sea and southward via the Deep Western Boundary Current (DWBC). The mean interior flow field in the Labrador Sea is found to play an important role in feeding both pathways. In particular, flow into the Irminger basin is due to a cyclonic recirculation located southwest of Greenland while the export via the DWBC is partially maintained through an internal pathway, transporting LSW across the basin to the west Greenland coast. A region of high eddy kinetic energy west of Greenland tends to increase the flushing rate of LSW, but its impact is found to be limited. The residence time for LSW in the Labrador basin is estimated to be approximately 4–5 years, with 80% leaving via the DWBC and 20% via the Irminger pathway.

Keywords: Deep-convection; Advection–diffusion model; Lagrangian floats; Labrador Sea Water; Labrador Sea; North Atlantic

1. Introduction

Labrador Sea Water (LSW) is an intermediate water mass (characterized by a salinity and potential vorticity minimum) produced by deep convection in the Labrador Sea—the northwest extension of the subpolar gyre. Formation occurs primarily in the sea's interior over a relatively small area (with diameter varying between 100 and 300 km; see Lab Sea Group, 1998). Once formed, LSW spreads far beyond its formation region and can be tracked throughout the entire North Atlantic, in both the subtropical and subpolar gyres, and as a constituent water mass of the mid-depth meridional overturning circulation. Three primary pathways for LSW spreading were proposed by Talley and McCartney (1982) through the mapping of the low potential vorticity associated with the weakly stratified LSW: southward in the Deep Western Boundary Current (DWBC), northeastward into the Irminger Sea, and into the eastern North Atlantic across the mid-Atlantic ridge towards the Iceland Basin and Rockall Trough. Since then, these pathways have been supported by a number of hydrographic and tracer

☆This is Woods Hole Oceanographic Institution Contribution No. 10714.

*Corresponding author.
E-mail address: fstraneo@whoi.edu (F. Straneo).

0967-0637/03/$ - see front matter
doi:10.1016/S0967-0637(03)00057-8

observations (e.g. Sy et al., 1997; Rhein et al., 2002).

While the spreading of LSW beyond the Labrador basin is relatively well-documented, the limited number of observations within the Labrador Sea itself provide relatively little information about the mechanisms by which it leaves the sea's interior. It has been conjectured that the transport of convected water away from the formation site is carried out by baroclinic eddies resulting from the collapse of the convective structure (see Marshall and Schott, 1998, for a review). This assumption, generally thought to apply to most convective sites, rests on two facts. First, baroclinic eddies containing newly ventilated water have been detected during, or shortly after, convection at a number of convection sites (Gascard and Clarke, 1983; Gascard, 1978) Second, numerical and laboratory studies of localized convection show the collapse of the dense water dome through baroclinic instability of the rim current at the edge of the formation region (e.g. Hermann and Owens, 1993; Maxworthy and Narimousa, 1994, and the review by Marshall and Schott, 1998).

Recent observations and modeling studies, however, indicate that the above scenario may not be the only mechanism responsible for the export of the dense water and for the restratification of the convective region. For example, hydrographic data collected during a recent wintertime survey of the Labrador Sea did not show evidence of a rim current at the edge of the convected region (Pickart et al., 2002). Furthermore, a significant fraction of the eddies present in the Labrador Sea's interior appear to originate from instability of the boundary current off the west Greenland coast (Lilly et al., accepted for publication; Prater, 2002). Finally, Straneo and Kawase (1999) argue that the baroclinic collapse scenario is artificially favoured in model simulations where convection is forced by means of a localized, discrete forcing. The uncertainties in the mechanisms responsible for the export, however, are not limited to the origin of the eddies. Recently, a high resolution float survey of the subpolar North Atlantic has identified a series of internal recirculations (Lavender et al., 2000) in a region previously thought to be mostly quiescent. This finding has raised the question as to what role such recirculations may play in the removal of LSW and, in particular, what the relative contribution of advection by this interior flow versus diffusion due to eddies is. Addressing these questions is particularly relevant to the understanding of the mid-depth component of the meridional overturning circulation, and for the interpretation of the far-field LSW observations—for example within the DWBC (Molinari et al., 1998), and in the subtropical gyre (Curry et al., 1998).

Data collected over the last few years, including that from the Labrador Sea Deep Convection Experiment (Lab Sea Group, 1998), have provided us with the unique opportunity of addressing these questions through basic modeling that is constrained by observations. Such is the approach taken in this study. We combine data collected by a large number of floats released in the Labrador Sea and neighboring regions with hydrographic data obtained during the winter of 1997 to construct an advective–diffusive model for LSW spreading at mid-depth. The mean velocity field and eddy diffusivity in the model are derived from the Lagrangian dataset, while the source location and amount of LSW formed is derived from hydrographic data.

2. The advection–diffusion model

2.1. Strategy of the model

We analyze the spreading of LSW through the evolution of a passive scalar quantity (i.e. one that does not affect the velocity field) which we refer to as 'LSW tracer' (LSW hereafter). Its mean evolution is described by an advection–diffusion equation,

$$\frac{\partial C}{\partial t} + \mathbf{U}(\mathbf{x}) \cdot \nabla C(\mathbf{x}, t) = Q(\mathbf{x}, t) - \nabla \cdot \mathbf{E}(\mathbf{x}, t), \qquad (1)$$

where $C(\mathbf{x}, t)$ is the tracer concentration per unit area ($\mathbf{x} = (x, y)$), $\mathbf{U}(\mathbf{x})$ is the mean stationary velocity, $Q(\mathbf{x}, t)$ is the mean source of LSW, and $\mathbf{E}(\mathbf{x}, t)$ represents the eddy fluxes of tracer (i.e. $\overline{\mathbf{u}'C'}$). A description of how the mean velocity and

eddy flux fields are derived from the float data, of the associated errors, and of the independent support for these derived quantities, can be found at the end of this section.

Before we proceed with the model description, it is important to review some of the basic assumptions behind the use of a barotropic advection–diffusion model to address LSW spreading. Because of the passive tracer assumption, the model is more appropriately suited for simulating the spreading of inactive tracers such as CFCs (introduced into the water column by convective mixing of the surface waters) than for tracking the low potential vorticity water formed by convection. However, two considerations support the passive tracer hypothesis for LSW spreading. First, the vertical stratification in the subpolar regions is limited and the flow field in the Labrador basin is mostly barotropic (as confirmed, for example, by the small difference in the flow field as inferred from the 400, 700 and 1500 m floats described in Lavender et al., 2000). Second, departures from the barotropic flow can be described mostly in terms of a two layer system—a surface layer and a LSW layer (below these is a layer of stratified overflow water which we assume not to affect LSW spreading). If we assume that the baroclinic flow field is geostrophic, then it will tend to be along the LSW (low PV) contours and hence cannot advect tracer across them. In this study, then, the spreading of LSW is governed by horizontal processes alone and its description is essentially reduced to a two-dimensional problem.[1] Having said this, we still recognize that this model is clearly a simplification of what is a much more complex dynamical problem, and any dynamical interaction between the flow field and the low potential vorticity, convected water must be addressed with more sophisticated tools. The goal of this study, however, is not a full dynamic simulation of LSW spreading but rather to make use of the flow field derived from floats (at this time the most accurate observational realization of the mid-depth mean flow in the subpolar North Atlantic) to investigate the export of LSW.

[1] This is consistent with LSW being formed via vertical convective mixing since the short timescale over which convection occurs (order of a week) enables us to decouple this from the much slower spreading process.

2.2. The mean velocity field

2.2.1. Derivation

The mean velocity field used in this study is obtained from over 200 Profiling Autonomous Lagrangian Circulation Explorer (PALACE) and Sounding Oceanographic Lagrangian Observer (SOLO) floats released in the North Atlantic during the period 1994–1998 (Lavender et al., 2000). These are quasi-Lagrangian, isobaric floats which periodically surface to transmit their position, and other data, to the Argos Satellite System. To construct the 700 m mean velocity field, Lavender et al. (2000) used floats from three levels: 400, 700 and 1500 m. The cycle time of the floats was 4.5 days (22%), 9 days (67%) or 19 days (11%), where percentages represent the fraction of floats with that cycle time. For each float one can calculate a displacement between every two surfacing events and then derive an approximate mean Lagrangian velocity from each displacement. These velocities were spatially and temporally averaged in cells roughly 100 km × 100 km, with each measurement weighted according to the time the float spent in the cell. The averaged field was then objectively mapped assuming a Gaussian covariance function for pressure with a decorrelation length scale of 185 km. The velocity covariance was deduced from the pressure covariance using the geostrophic relation. The reader is referred to Lavender (2001) and Davis (1998) for a description of the method.

The inferred Eulerian velocity field has a weak net outflow across the southern boundary, which must be corrected in order to run the advection–diffusion model. We do this by applying a uniform adjustment (3.5 mm/s) to the velocity field at the open southern boundary. The model results proved to be independent of whether the correction was applied to the eastern or southern open boundaries. The resulting non-divergent flow field is then obtained by computing the vorticity for the boundary-corrected, objectively analyzed field, and inverting it with a Poisson solver to obtain the streamfunction field (see Fig. 1). The mean

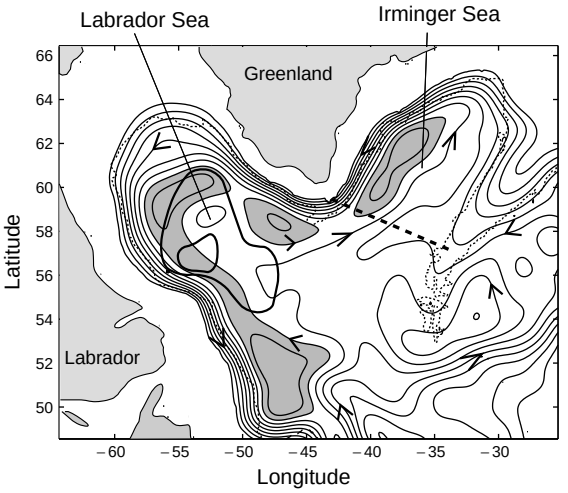

Fig. 1. Streamfunction field derived from the float data after applying the non-divergence correction. The shaded grey areas indicate the series of cyclonic recirculations. The thick black contours denote the area of LSW formation for a high (large area) and a low (small area) convection year. Overlaid (dashed) is the 2000 m isobath. Arrows indicate the direction of flow. The tracer flux into the Irminger Sea is calculated across the straight dashed line.

flow is only marginally different from the original Eulerian mean field of Lavender et al. (2000), and all structures present in the streamfunction field can also be found in the original velocity field. Apparent in the streamfunction field is the large scale cyclonic circulation of the subpolar gyre, the sub-basin scale cyclonic recirculations in the interior, and a somewhat diffuse North Atlantic Current in the south eastern corner of the domain.

2.2.2. *Assumptions and errors in the mean field*

Implicit in the formulation of (1) is a separation between the mean and fluctuating components of the flow. It is reasonable to assume that the turbulent time and space scales relevant to the spreading of LSW within the subpolar gyre are those of the eddies present in the interior of the Labrador Sea. Hence, for the floats to correctly sample the mean flow, their displacements must be averaged over timescales longer than the typical eddy timescale. If the floats were truly Lagrangian, estimates of the latter could be obtained directly from the float data. However, because of the periodic surfacing of the floats, we instead estimate the eddy timescale from observations of eddies at the Bravo Mooring site, located in the central Labrador Sea. These show the existence of two kinds of eddies: those formed via the convection process and those originating from the West Greenland boundary current (Lilly et al., accepted for publication). The former are smaller, with radius 5–15 km and velocities 10–30 cm/s, while the latter are larger, with radius 15–25 km and velocities between 30 and 80 cm/s. If we take the smaller velocity range as a lower estimate for eddy velocities at 700 m, then an upper estimate for the time it takes a parcel to go around an eddy is 4–10 days. An alternative estimate for the integral Lagrangian timescale, T_L, is obtained as follows. T_L is defined as the ratio of the integral Lagrangian lengthscale, L, and the rms eddy velocity. We now make the assumption that L is approximately constant over the region of interest so that T_L is inversely proportional to the rms eddy velocity (see Zhang et al., 2001 for a review of all float data in the North Atlantic supporting this assumption). The value of L is chosen to be 20 km, in agreement with the eddies observed by Lilly et al., discussed above, but also as measured from isopycnal floats in the subpolar North Atlantic (Zhang et al., 2001). Given an rms eddy velocity measured from PALACE floats at 700 m in the Labrador Sea region that varies between 3 and 6 cm/s, T_L is estimated to vary between 3.8 and 7.7 days. We take this estimate to be representative of a Lagrangian Integral Timescale at the 700 m depth range for the Labrador Sea and, since floats were cycling predominantly at 9 days or beyond, it is reasonable to assume that successive displacements are uncorrelated and that they are effectively averaging over the eddies.

For Lagrangian floats to accurately sample an Eulerian mean field, the latter must be non-divergent and the float distribution must be spatially uniform (Davis, 1991). Because the mean field was estimated assuming the geostrophic relation, the field is non-divergent (within mapping error). The majority of floats were released in the western Labrador Sea in the region of deepest convection. This non-uniformity in float distribution introduces a bias (known as 'array bias') in

the velocity measurements due to the down-gradient flux of particles associated with the eddy field. Following Davis (1991, 1998) this bias can be estimated as

$$U_{j,\text{array}} = -\kappa_{jk}\frac{\partial \ln N}{\partial x_k},$$

where $j,k = 1,2$ and summation is implied over repeated indices, $N(\mathbf{x})$ is the number of independent observations per bin, and $\kappa_{jk}(\mathbf{x})$ is the eddy diffusivity (see Section 2.3). As to be expected, there is a net velocity bias out of the region where the floats were deployed. However, its magnitude[2] is limited to a few mm/s in the interior and hence is small compared to an interior flow of several cm/s. In boundary current regions the array bias increases to larger values (a few cm/s), but even here it is small when compared to the typical boundary current velocities of approximately 10 cm/s. We conclude that the error introduced in the mean field by the array bias can be neglected.

The standard error $\sigma_{\bar{u}}$, associated with the limited length of the record, is defined as the rms velocity variance divided by the square root of the number of independent observations (calculated following Owens (1991), using a correlation time of 10 days). As shown in Fig. 2, the sampling error computed as such is relatively small throughout the domain, with the exception of the region south of 50°N, which is dominated by the North Atlantic Current. The large eddy variability in that region, together with the limited float sampling, did not allow for an accurate determination of the mean flow. As will become apparent later, however, the results discussed in this study are independent of the features present in the region of the North Atlantic Current.

Finally, there is the issue of whether the floats were sampling a particular phase of the circulation in the subpolar gyre. The floats were launched between 1994 and 1998 during a transition between a high convection and a low convection period—which roughly coincided with the end of a high North Atlantic Oscillation (NAO) phase and the start of a low NAO phase. Since changes in the North Atlantic circulation have been associated with changes in the NAO pattern (e.g. Dickson et al., 1996; Curry and McCartney, 2001), it is possible that the mean circulation observed by the floats is biased towards the low NAO phase.

[2] Estimated by using an upper limit for κ of 10^7 cm^2/s (see Section 2.3).

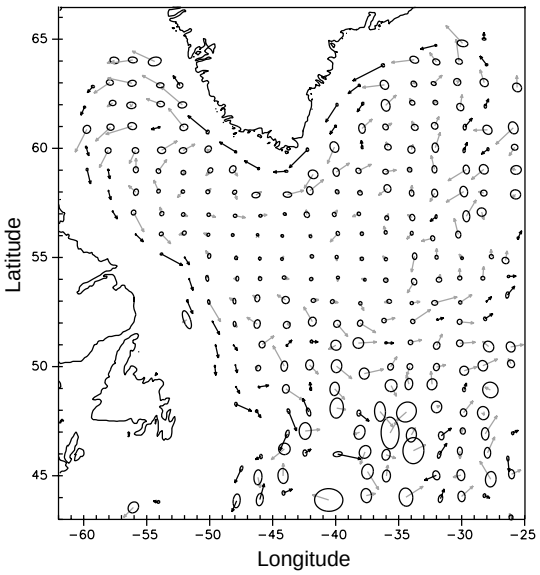

Fig. 2. Sampling error ellipses overlaid on the mean Eulerian velocity field measured by the floats. Black arrows show displacements over 30 days for speeds above 5 cm/s, and grey arrows for speeds below 5 cm/s.

2.2.3. *Independent support for the mean flow field*

As discussed in Lavender et al. (2000), the recirculations close to the boundaries (Fig. 1) are essentially newly discovered features that have emerged from the float data. Support for the westernmost recirculation, close to the coast of Labrador, is found in Fischer and Schott (2002). The southern portion of the recirculation (south of 53°N and north of Orphan Knoll) is present in the mean velocity field (at 1500 m) derived from their independent set of PALACE floats (three floats actually leave the equatorward flowing boundary current and circle back north). Furthermore, LADCP sections (one at 53°N shown in their figure 4) indicate a weak anticyclonic recirculation adjacent to the southeastward flowing boundary current. Finally, this same interior northwestward flow, is seen in the 2-year mean 1500 m current

meter record on a mooring offshore of the boundary current located again at 53°N. The magnitude of this mean northwestward flow observed at the mooring (2.4 cm/s) is in agreement with the mean velocity derived from the PALACE floats of Lavender et al. (2000) for this region (2 cm/s). Note that the LADCP section showed northwestward velocities of up to 5 cm/s but, given the synoptic nature of the LADCP measurements and the time and space smoothing of the float data, such a value is not inconsistent with the float data. Further to the north, this same recirculation is supported by the hydrographic observations of Clarke and Gascard (1983) and Pickart et al. (2002), showing that offshore of the western boundary current (around 56°N) lies the region where the deepest wintertime mixed-layers have been observed. These observations are consistent with the notion of preconditioning due to a weak cyclonic circulation as discussed in Clarke and Gascard (1983). Surface drifter data supports the existence of all three recirculations (see Cuny et al., 2002, for a discussion of the two recirculations in the Labrador Sea; and Jakobsen et al. (in press), for all three). These appear both in the Eulerian mean maps and in the drifter's trajectories. From these studies, however, it is difficult to tell whether the two recirculations on either side of Greenland are connected or not.

The model of Käse et al.'s (2001), a 1/6° resolution regional numerical model of the subpolar North Atlantic and Nordic Seas, forced with daily flux fields for 1992–1997, shows essentially the same features in the 700 m velocity field as the mean Eulerian velocity field used in this study. The velocities in their model, however, tend to be approximately double those recorded by the floats. Further evidence for the interior anticyclonic circulation, found in the central Labrador Sea, can be found in the barotropic streamfunction field of Smith et al. (2000) basen on their 1/10° numerical model of the North Atlantic. Finally, support for the existence of sub-basin scale recirculations on either side of Greenland is found in the recent modeling study of Spall and Pickart (in press), who show how they can be generated by localized, seasonal wind forcing.

2.3. The eddy diffusivity

2.3.1. Derivation

Lateral mixing due to mesoscale eddies, in this advection–diffusion model, is parameterized as an eddy diffusivity. The derivation of an Eulerian eddy diffusivity from float data is discussed by Davis (1987), who generalizes Taylor's (1921) single particle diffusivity to inhomogeneous and non-stationary conditions. Davis derives a generalized advection–diffusion equation for the spreading of a passive tracer, in which the eddy fluxes can be described in terms of the mean tracer concentration and of the Lagrangian diffusivity (κ_{ij}) from floats in the random-walk regime,

$$E_i(\mathbf{x},t) = \langle u_i'(\mathbf{x},t)C'(\mathbf{x},t)\rangle = -\kappa_{ij}(\mathbf{x})\frac{\partial C(\mathbf{x},t)}{\partial x_j}, \quad i,j=1,2,$$

provided that two main conditions are satisfied. First, measurements must be uncorrelated—which means that the Lagrangian diffusivity of the floats has approached the random-walk-regime asymptotic value and hence is time independent. Analysis of Lagrangian float data show that this generally holds for times greater than the Lagrangian integral timescale, T_L (Colin de Verdiere, 1983; Krauss and Böning, 1987). Following the discussion in Section 2.2, given the eddy scales observed in the Labrador Sea and the float cycling time, we assume that successive float displacements are uncorrelated and that the measurements are independent. The second condition is that the tracer concentration must vary slowly over T_L, which is a reasonable assumption everywhere in our study domain except for the boundary current region. In this region, however, it is safe to assume that diffusive effects are small compared to the advection.

Assuming then that we are in a regime in which Davis's generalized advection–diffusion equation holds, the two diagonal components of the eddy diffusion tensor (the symmetric diffusion tensor) that dominate the lateral mixing[3] are equal to the

[3]The two off-diagonal components are assumed to be negligible, in agreement with the direct measurement of κ_{xy} from North Atlantic float data (LaCasce and Bower, 2000), and

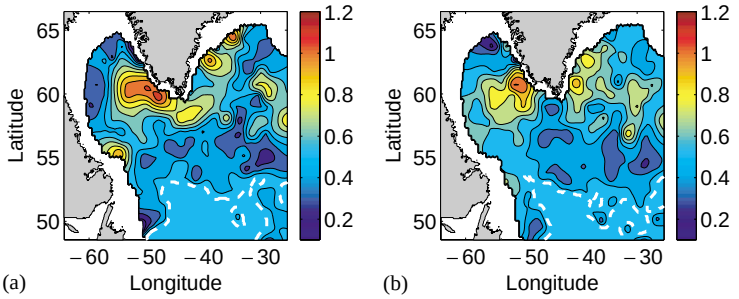

Fig. 3. Eddy diffusivities (10^7 cm^2/s) calculated using equation (2) with a Lagrangian lengthscale of 20 km. (a) Zonal diffusivity; (b) Meridional diffusivity. Dashed white contour indicates the area within which the diffusivity is set to a background value of 0.6×10^7 cm^2/s, contour interval is 0.1.

Lagrangian diffusivity, defined as

$$\kappa_{ii}(\mathbf{x}) = L_i\sqrt{\overline{u_i'^2}}, \tag{2}$$

where $i = 1, 2$ represent the zonal and meridional directions and L_i is the integral Lagrangian lengthscale.[4] Because of the floats' profiling nature, the Lagrangian diffusivity cannot be directly calculated from the float data. Instead we make the assumption that the Lagrangian lengthscale in the region is approximately constant, so that (2) reduces to the product of a spatially constant Lagrangian lengthscale and the zonal and meridional floats' variance. Such an approximation finds support in a number of float studies that explicitly calculate both the diffusivity and the integral Lagrangian space and time scales in various mid-latitude oceanic regions (Krauss and Böning, 1987; Schäfer and Krauss, 1995; Zhang et al., 2001) and by a comparison of mid-latitude float data from different regions (Böning, 1988).

One last issue to be addressed involves the anisotropy in the Lagrangian lengthscales found in a number of mid-latitude float studies ($L_x > L_y$; Colin de Verdiere (1983), Krauss and Böning (1987), and Schäfer and Krauss (1995)). This has been attributed to the suppression of meridional spreading due to the β-effect. Because of the smallness of β at high-latitudes, however, in this study we assume that the Labrador Sea is characterized by a single, isotropic, Lagrangian lengthscale. Its value is set to 20 km, in agreement with the size of eddies observed in the Labrador Sea (Lilly and Rhines, 2002). Given a constant L, and since the rms eddy velocities of the floats released in the Labrador Sea are very nearly isotropic (i.e. $\overline{u'^2} \approx \overline{v'^2}$), the resulting zonal and meridional components[5] of the eddy diffusivity are very nearly identical (Fig. 3). Because the North Atlantic Current region was undersampled by floats, we chose to set the diffusivity in this region to a mean background value of 0.6×10^7 cm^2/s. This was done by setting all values larger than this background to this value in the region bound by the same contour (Fig. 3). Prior to smoothing, the rms eddy velocities had maximum amplitudes of 8 cm/s and an average value of 4.5 cm/s if averaged over this area, to be compared with a mean velocity that never exceeded 6 cm/s. As shown by the error ellipses in Fig. 2, the floats clearly undersampled this region that is dominated by the northwest corner of the NAC and it is impossible, from this dataset, to determine whether the large rms eddy velocities represent instabilities (and eddy formation) or simply meandering of a fast current. By setting the diffusivity in

(*footnote continued*)
with the fact that the cross-correlation rms eddy velocity ($\overline{u'v'}$), from the floats utilized in this study, is an order of magnitude smaller than $\overline{u'^2}$ and $\overline{v'^2}$, (see also Davis, 1991).

[4] An equivalent definition in terms of the integral timescale, T_i, can be obtained by substituting $L_i = T_i\sqrt{\overline{u_i'^2}}$.

[5] The corresponding rms eddy velocities (in cm/s) can be obtained by dividing κ by 20×10^5 m.

this region to a background value, we are likely damping any active mixing in this region. As discussed later this does not affect the export pathways out of the Labrador Sea (that are the focus of this study) but may affect possible return pathways for Labrador Sea Water. For example, it is quite possible that a second pathway into the eastern North Atlantic may result from LSW flowing south in the DWBC and being then entrained by the deep portion of the NAC and advected eastward. Such a pathway will not be resolved in this study. Excluding this region, the maximum amplitude of the rms eddy velocities are found off of the West Greenland coast and are on the order of 6 cm/s.

2.3.2. Independent support for κ

The diffusivity in Fig. 3 shows a relatively large spatial variability. The most prominent feature is the eddy kinetic energy (EKE) maximum found off of western Greenland. There is now extensive observational support for this feature both in surface data (drifter data—Cuny et al., 2002, Jakobsen et al. (in press); altimeter data—Lilly and Rhines, 2002, and Prater, 2002) and in subsurface data, where this maximum is visible at all three depths sampled by the PALACE floats. The EKE maximum also appears in the numerical simulations of Smith et al. (2000) and Käse et al. (2001).

In terms of the relative magnitude of the eddy diffusivity, ideally one would want to verify our estimate against those obtained by analyzing the dispersion of Lagrangian floats at comparable depths in other high-latitude regions. Because of the limited number of such studies, however, such a comparison is currently not possible. Nonetheless, we can say that the order of magnitude of the diffusivity derived in this study is at least consistent with other mid-depth estimates for low to medium eddy activity regions (see Zhang et al., 2001, for a review of κ values derived from float dispersion for the North Atlantic). Finally, by assuming that the restratification of the Labrador Sea is carried out by an eddy-driven secondary circulation, Khatiwala et al. (2002) estimate an implied $\kappa = 0.3\text{–}0.6 \times 10^7\ \mathrm{cm^2/s}$ from hydrographic data.

2.4. Location of LSW formation

Because of the large interannual variability in the amount of LSW formed (e.g. Lazier, 1995), we will show results from two convection scenarios: a low formation year and a high formation year. The low convection scenario is based on wintertime hydrographic observations from 1978 (Clarke and Gascard, 1983) and 1997 (Pickart et al., 2002). These were mild to moderate winters in which convection was limited to a fairly small patch (approximately 150 km in diameter, Fig. 1). During more severe winters convection can occur over a greater area (e.g. Pickart et al., 1997). Because three-dimensional surveys of the entire Labrador Sea are rare, the exact area of the convective patch during high convection years is unknown. However, from the 1997 wintertime survey, Pickart et al. (2003) calculated that with two more weeks of buoyancy loss, convection would have occurred over a patch of approximately 250 km in diameter, (Fig. 1).

For addressing the low and high convection scenarios, the tracer concentration is set to a constant value of one over the 'convected patch' in both cases. We make this choice for reasons of simplicity, and the results derived are not sensitive to this choice provided no quantitative comparison is made between the high and the low scenario values. If the tracer concentration were to reflect the actual volume of LSW formed, then a low convection scenario would also be characterized by a shallower convective layer compared to the high convection case. The areas of the low and high convection patches are in a ratio of approximately 1–10. This is consistent with the estimates of LSW formation from CFC data presented by Rhein et al. (2002). They estimate a formation rate of 8.1–10.8 Sv during the high convection period of 1988–1994, and a much smaller formation rate of 1.8–2.4 Sv for the low convection period of 1995–1997.

2.5. Boundary conditions and parameters

The domain for the advective-diffusive model integrations is shown in Fig. 1. It includes an open-boundary over a fraction of both the

southern and eastern boundaries. Here tracer is allowed to advect and diffuse out of the domain, while the tracer flux back into the domain is assumed to be zero. There is no advection or diffusion of tracer normal to the topographic boundaries. The grid spacing in our model simulations is 10 km × 10 km, and the time step is 72 min. The model employs a staggered grid in velocity and tracer concentration. Time-stepping is centered-difference in time, with advection of tracer represented by a third-order upwind scheme (Holland et al., 1998). Diffusion of tracer is described by a third-order centered-difference scheme.

3. Spreading of Labrador Sea Water

The model described above is meant as a tool for understanding and exploring those processes that lead to LSW spreading away from the formation region, and of the timing involved. LSW, in this context, is simulated via the release of a passive dye in the interior of the Labrador basin. Mixing of tracer due to eddy action is represented via a downgradient diffusion of tracer through a Laplacian operator. The directions and rates of LSW spreading are thus determined by the interplay of features such as the interior flow, the boundary current, and the spatially heterogeneous eddy diffusivity. We investigate the individual impact of each of these features by running the model in different configurations (achieved through modification of the eddy diffusivity field alone), each emphasizing a single feature at a time. Given the uncertainties in estimating the eddy diffusivity, and in determining the magnitude of the mean flow, our goal is also to present a series of possible scenarios for LSW spreading—spanning the range of realistic possibilities.

3.1. The advective and diffusive pathways

As mentioned above, the recirculations revealed by the PALACE floats in the interior of the Labrador Sea are new features. What is the impact of these recirculations, if any, on the dispersal of LSW? A first step in addressing this question is to estimate the relative importance of advection versus diffusion in the interior region. This ratio is given by the Peclet number, $P = UL_c/\kappa$, where κ is the diffusivity from Section 2.3 and L_c is a characteristic length scale (100 km, the width of the recirculations). Computed as such, P indicates that advection dominates in the boundary current region, while it is comparable to diffusion in the interior (Fig. 4). To distinguish between the effects of diffusion and advection, given they are of comparable magnitude in the interior, we first ran the model in the extreme limits of low and high diffusivity, adv and diff, emphasizing advection and diffusion separately. For simplicity, κ is assumed to be spatially homogeneous in these runs with values set to 0.1×10^7 cm^2/s in the advective limit, and 10^7 cm^2/s in the diffusive limit.

Three distinct advective pathways for the transport of tracer are evident in the advective limit, adv (Fig. 5). Two of these are responsible for the advection of tracer out of the Labrador basin—a DWBC pathway, and an Irminger pathway, while the third is an internal pathway responsible for the advection of tracer within the basin (Fig. 6). The DWBC pathway is initially fed by tracer released directly into, or close to, the boundary current off the Labrador coast. Subsequently, the DWBC export consists of tracer released farther offshore of the boundary current, which diffused or advected into it, and then was carried around the basin. The Irminger pathway, which transports

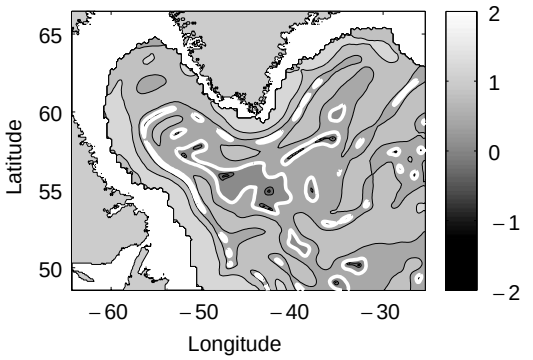

Fig. 4. Logarithm (base 10) of the Peclet number, defined as UL/κ, where U is the local speed, κ is the average of the zonal and meridional diffusivities, and L is taken to be 100 km. The thick white contour indicates the zero contour, contour interval is 0.5.

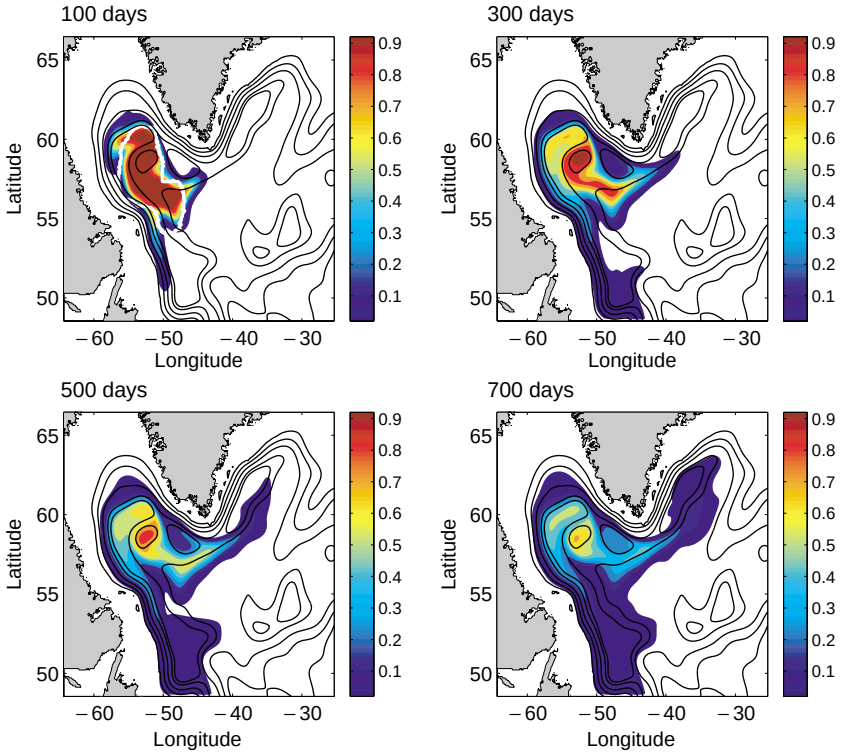

Fig. 5. Tracer concentration at different times for the advective run, adv (high convection scenario). Contours are the same for all panels (cont. int. is 0.1), streamlines are overlaid in black. Overlaid on the first panel is the outermost contour of the initial tracer distribution (white).

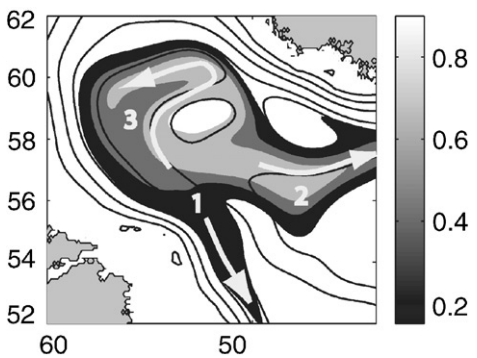

Fig. 6. Detail showing tracer concentration at day 300 for adv (in the high convection scenario), contour interval is 0.25. The three advective pathways are indicated by grey arrows; (1) DWBC, (2) Irminger Pathway, (3) internal pathway. Streamlines are in black.

tracer eastward into the Irminger Sea, is fed by the cyclonic recirculation located southwest of the southern tip of Greenland. Once in the Irminger Sea, in this advective limit, tracer is then wrapped around the Irminger's cyclonic recirculation (Fig. 5). The third, and new, advective pathway is found in the interior of the Labrador sea. It is an 'internal' pathway, due to the northernmost recirculation, which transports tracer from the center of the basin to the west Greenland coast (roughly towards 59°N, 51°W, Fig. 6). After reaching the Greenland coast, tracer is then diffused into the boundary current and advected cyclonically out of the basin via the DWBC route. Finally, we see how the westernmost recirculation is responsible for tracer leaving the boundary current in the Flemish Cap area (around 50°N, 45°W, Fig. 5) and recirculating to the north back towards the Labrador basin. This pathway is consistent with the observations of PALACE floats leaving the boundary and moving northward discussed by Lavender et al. (2000) and Fischer and Schott (2002).

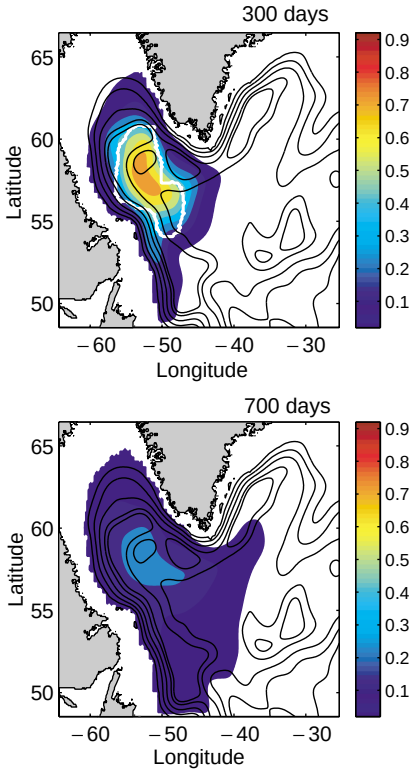

Fig. 7. Tracer concentration at 300 and 700 days for the diffusive run, diff (high convection scenario). Contours and overlaid fields are the same as for Fig. 5.

The role of the recirculations, so prominent in adv, diminishes as the eddy diffusivity value is increased. In diff, tracer tends to spread uniformly out of the region where it was released (Fig. 7) with advective effects being appreciable only in the boundary current. Note that the increase in κ contributes to a faster removal of LSW from the basin, as shown by the decreased amount of tracer remaining in the Labrador Sea at any given time when comparing adv to diff (Figs. 5 and 7).

3.2. The heterogeneous eddy diffusivity

Our next step is to investigate the extent to which the spatial variability in κ affects the spreading of LSW. The most salient feature of the eddy diffusivity field is the maximum off of the west Greenland Coast (near 60°N, 49°W, Fig. 3). The center of the maximum is located within the boundary current, but the region of high diffusivity extends over the northernmost recirculation of the Labrador Sea, and over the region where the boundary flow is decelerating over the broadening topography (Fig. 8). Such an inhomogeneous turbulence field will cause the center of mass of a localized tracer patch to move up-gradient of the turbulent field. In other words, LSW formed on the western side of the basin will tend to propagate eastward and, in particular, along the 'internal advective pathway' discussed above. The magnitude of this net flow is given by the gradient of κ (e.g. Freeland et al., 1975) and, given the κ derived in Section 2.3, its magnitude is limited to 1–2 mm/s. Since the mean flow in the interior of the basin is typically an order of magnitude greater than this, we anticipate that such upgradient motion is negligible with respect to the advection.

We first address the spreading of tracer in the presence of the spatially variable eddy diffusivity computed in Section 2.3 (Fig. 3) in run basic. As expected, the spreading of tracer in basic is caused by a combination of the advective and diffusive effects found in the two extreme runs discussed above (Fig. 9). To analyze the effects of the

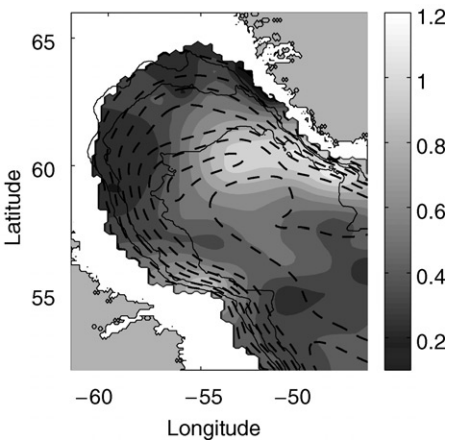

Fig. 8. Detail of the magnitude of the diffusivity (average of zonal and meridional κ, cont. int. 0.1×10^7 cm^2/s). Overlaid is the streamfunction field (black dashed contours) and the 1000, 2000 and 3000 m isobaths.

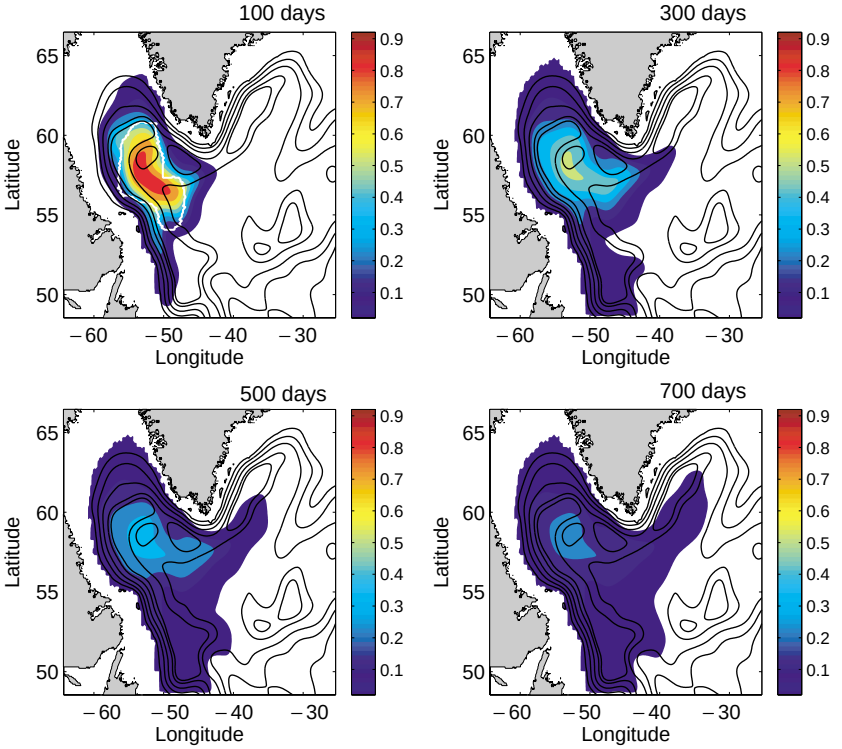

Fig. 9. Same as Fig. 5 but for run basic (high convection scenario).

diffusivity maximum in more detail, we compare the results of basic to those from hom, a run in which the maximum in κ is replaced by a background value of 0.6×10^7 cm^2/s (meant to represent the mean eddy diffusivity in the Labrador Sea if the maximum were absent). The overall tracer spreading in hom and basic is very similar—confirming the limited impact of the eddy diffusivity maximum. The maximum does, nonetheless, contribute to a more rapid removal of tracer from the sea's interior: less tracer remains in the interior and more tracer enters in the boundary current after 300 days (Fig. 10). Furthermore, by increasing the mixing off of the west Greenland coast, the diffusivity maximum enhances the flux of tracer into the Irminger basin by feeding the recirculation southwest of the tip of Greenland. In terms of amplitude, however, we find that the net difference in concentration between hom and basic is on the order of 10–20% of the total concentration. This in turn limits the impact on the net tracer flux to less than 5%. Hence, our conclusion is that the impact of the eddy diffusivity maximum is limited.

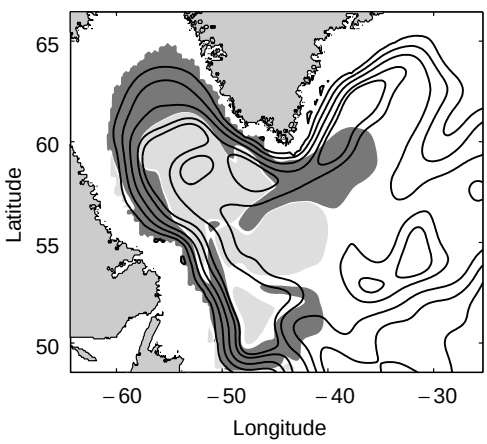

Fig. 10. Tracer concentration for basic minus hom, 300 days after tracer release (high convection scenario). Dark shading represents positive values and light negative values. Overlaid are the mean flow streamlines.

3.3. Tracer flux via the DWBC and Irminger pathways

The results presented so far have shown that the rates and pathways for the export of LSW vary with eddy diffusivity. To quantify such variations, we start by considering how the DWBC flux varies for the three main experiments, adv, basic and diff. The flux is calculated as the zonally integrated flux of tracer at the southern boundary, at approximately 50°N (Fig. 11). The broad features of the export flux are common to all three runs: it rapidly builds to a peak, then slowly decreases. The timing for the first peak, approximately 0.5 years after tracer was released, is the same for all three runs. This peak is due to tracer released in (or very close to) the boundary current and rapidly advected southwards. The varying magnitude of the peak reflects the different rate of tracer entering the boundary current off the Labrador coast through diffusion—consequently this is much larger for diff than for adv. After the first peak, the DWBC flux is due to tracer advected or mixed into the boundary flow around the perimeter of the Labrador basin. This gives rise to a long 'tail' slowly decreasing in amplitude with time. In the advective limit, however, there are a number of additional peaks beyond the first and, furthermore, the second peak is the strongest signal (occurring approximately 9 months after the first). This second peak results from tracer being transported across the basin via the internal advective pathway where it is then mixed into the boundary current. The diminishing amplitude of this peak, from adv to basic, is representative of the decreasing importance of the internal advective pathway as diffusive effects become dominant in the interior of the basin. Finally, the different areas beneath the curves show how, going from an advective to a diffusive regime, the rate of export of LSW via the DWBC increases considerably. This implies more rapid flushing of LSW in the diffusive limit; a result we will return to in Section 3.5.

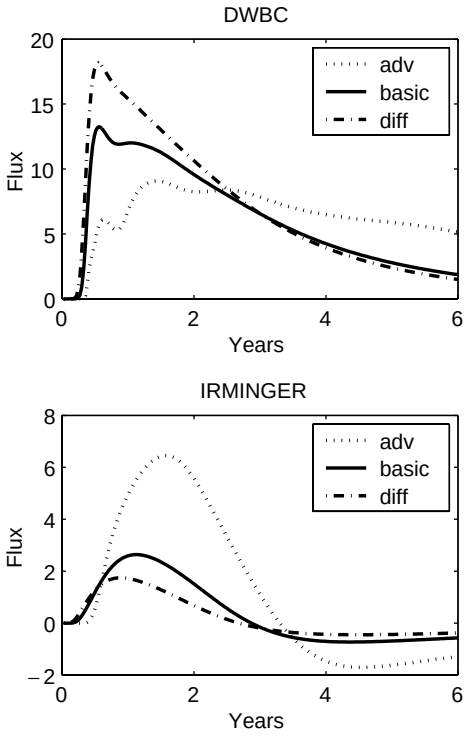

Fig. 11. Zonally integrated flux of tracer (in units of tracer concentration ($\times 10^7$ m^{-1} s^{-1})) as a function of time for runs adv, basic and diff: DWBC flux (top panel); Irminger Sea Flux (bottom panel).

The net amount of tracer flux into the Irminger Sea (computed across the line shown in Fig. 1) also varies with eddy diffusivity (Fig. 11). The flux reaches its maximum 1–1.8 years after the tracer release, depending on the diffusivity. It then decreases and eventually becomes negative, as tracer is advected out of the Irminger Sea via the boundary current on the eastern side of Greenland. The amplitude of tracer flux into the Irminger Sea is much larger in the advective run than for the others, reflecting how this pathway tends to be more favoured when transport of tracer across streamlines (i.e. diffusion) is reduced. The opposite is true for the DWBC pathway which relies, except for the tracer released in the boundary current, on diffusion of tracer into the boundary current. A more detailed analysis of the timing of the arrival of LSW in the Irminger Sea is found in Pickart et al. (2003).

3.4. The high and the low convection scenarios

Implicit in the passive tracer assumption is that the mean advective and diffusive fields do not vary

with a varying LSW distribution. As a result, any differences between a high and low convective scenario are limited to those resulting from the different areas over which LSW is initialized. All of the simulations presented so far have been the high convection scenario. In the low convection scenario, the smaller patch of tracer (Fig. 1) erodes faster than the high concentration patch, but its export is along the same pathways (not shown). Because the bulk of tracer in the low convection scenario is closer to the Labrador coast, the relative impact of the internal pathway is diminished. This results in a smaller amplitude second peak (with respect to the amplitude of the first) and a greater time delay between the two (on the order of 15 months) due to the greater distance the tracer has to travel before it can get to the eastern boundary current. Similarly, tracer arrives in the Irminger basin with a delay of approximately 1 year with respect to the arrival in the high convection case.

3.5. Partitioning and residence time

The two principal pathways for tracer export out of the Labrador Sea in these model simulations are into the subtropical North Atlantic, via the DWBC, and into the Irminger Sea, via the edge of the interior recirculations. In terms of the partitioning of LSW amongst these two different pathways, approximately 70% of the total amount of tracer leaves via the DWBC, while only 10–20% escapes into the Irminger Sea in the high convection scenario (Fig. 12). The amount of tracer in the Irminger basin reaches a maximum 2–3 years after it is released in the Labrador basin (Fig. 12, lower panel). As shown in Fig. 11, as the diffusivity is reduced a larger net amount of tracer is exported into the Irminger basin.

The cumulative DWBC export reaches a plateau after approximately 6–7 years in both the basic run and the diffusive run, while it takes approximately 10–12 years in the advective run. If we define the residence time of LSW as the amount of time it takes for $1/e$ of the total amount of tracer to leave the basin, then the residence time for the advective, basic and diffusive runs is approximately 6.7, 4 and 3.5 years, respectively,

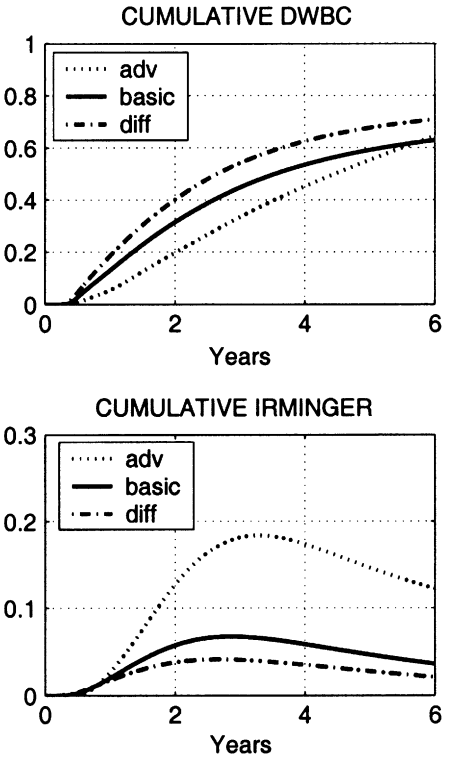

Fig. 12. Cumulative amount of tracer (expressed as a fraction of the total initial tracer amount) that has left the Labrador Sea via the DWBC (top panel), and that present in the Irminger Sea (lower panel) as a function of time. Shown are the adv, basic and diff runs (high convection scenario).

for the high convection scenario. The increase in residence time for the advective scenario is due to the difficulty, once diffusion is decreased, to export LSW away from its interior formation region.

In the low convection scenario the partitioning tends to favor the DWBC export route, with up to 80% leaving via this pathway. The net flux into the Irminger basin is accordingly reduced (not shown). This can be attributed to the westward shift in the center of mass of the initial LSW distribution in the low convection case with respect to the high convection case. The residence times in the low convection scenario are slightly lower than for the high convection scenario, since the center of mass of the tracer is located closer to the DWBC, but only by a few months.

4. Realistic eddy diffusivity: a comparison with data

Until now, we have used the model to describe the spreading of LSW in three different regimes: an intermediate diffusivity (basic, using the κ derived in Section 2.3), a low diffusivity (adv) and a high diffusivity (diff). This approach, as mentioned above, was motivated by the inherent uncertainty associated with estimating an eddy diffusivity. By comparing our results with observations, we now argue that the model has been successful in reproducing LSW spreading and that the diffusivity which best agrees with observations is in the low to intermediate range (i.e. experiments adv and basic).

4.1. The pathways

The three spreading pathways of LSW initially described by Talley and McCartney (1982), were inferred from a lateral distribution of the mid-depth LSW PV minimum, constructed from hydrographic data collected mainly between 1957 and 1962. The distribution is reproduced here as Fig. 13a. This time period coincided with a period of moderate convection. A second map (Fig. 13b) was constructed from data collected between 1966 and 1967 following a period of low convection (Lazier, 1973; I. Yashayaev, personal communication, 2001). The PV distribution during the latter period still shows a pool of low potential vorticity in the Labrador Sea, but such pool is now detached from the western boundary and slightly shifted to the southeast.

In order for the Irminger pathway to be discernible, diffusion must be lower than that used in diff. This suggests that mixing effects in the region are best represented with a low to medium diffusivity. Furthermore, we now argue that in the adv (not shown) and basic set-up, the model is capable of qualitatively reproducing both LSW distributions discussed in Talley and McCartney (1982), provided the history of tracer release is made to mimic the conditions described above. We simulate the 1958–1962 period by releasing tracer in the high convection region for four consecutive winters. By contrast, the 1966–1967 period consists of a single (high convection region) tracer release

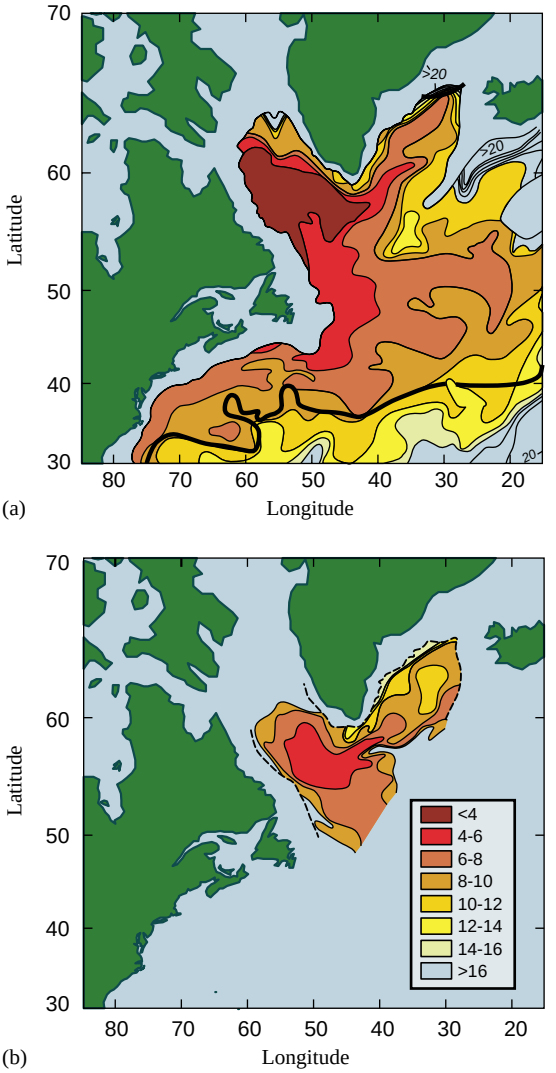

Fig. 13. Potential Vorticity maps at the LSW level for two different periods (from Talley and McCartney, 1982): (a) 1957–1962; (b) 1966–1967.

during the first winter only. Contour maps for tracer concentration after 4 years are shown in Fig. 14. As we already know, the model is effective in reproducing the 1958–1962 pathways discussed in Talley and McCartney (1982), with the exception of the poorly resolved pathway into the eastern North Atlantic (Fig. 14a). Since the North Atlantic Current is not realistically represented by the model, we would not expect to properly resolve

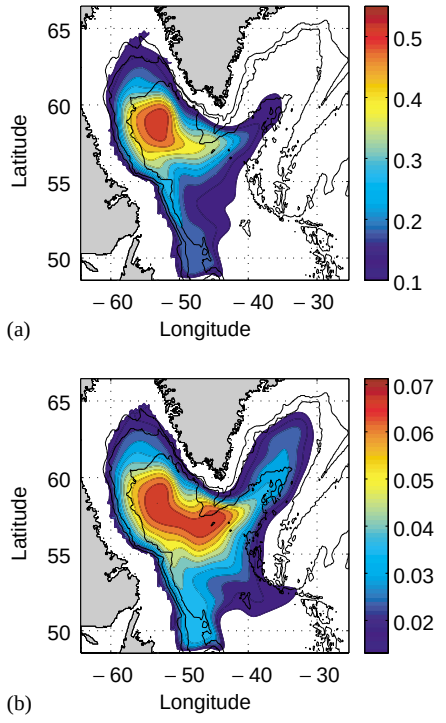

Fig. 14. Tracer concentration after 4 years for (a) a repeated yearly high convection tracer release; (b) a single high convection release during year 1. Contour values are chosen so that the range shown for both (a) and (b) has the same e-folding length.

this third pathway. As seen in Fig. 14, the model is also qualitatively successful in describing the spreading following the minimal convection period of 1966–1967. The LSW core is gradually eroded by advection out of the region via the boundary current, and what remains slowly migrates towards the center of the subpolar gyre, south of Greenland, by a combination of advection along the Irminger pathway and diffusion. The center of the remaining core thus shifts from the western Labrador Sea to the southwest of Greenland (Fig. 14b), in agreement with the observations presented by Talley and McCartney (Fig. 13b). Overall, then, the model is qualitatively able to reproduce both convection periods, provided the diffusivity is not too high.

In the basic and adv runs, we showed the existence of an internal advective pathway, transporting tracer from the interior to the west Greenland coast (this pathway disappears in the diffusive limit). There is presently no direct evidence for the existence of such a pathway, though some PALACE float trajectories appear to follow such a route (e.g. Lilly et al., 1999, and Lavender et al., 2000).

4.2. The spreading timescales

We estimated the residence time for LSW in the Labrador basin to be on the order of 4–5 years (Section 3.5). This estimate is supported by recent hydrographic data collected in the Labrador Sea showing that the volume of cold and fresh LSW, produced as a result of strong convection in the early 1990s, was nearly depleted approximately 4–5 years later (J. Lazier, 2001, personal communication). Regarding spreading timescales, Sy et al. (1997) use hydrographic and tracer data to suggest that LSW can arrive in the Irminger basin within 6 months. As the authors themselves admit this would require a mean advective velocity of 4.5 cm/s from the western Labrador Sea to the Irminger Sea. Even in the high convection scenario, where LSW formation occurs close to the Irminger basin, we found that it takes over a year for any significant amount of LSW to reach the basin. In fact, according to our simulations, the time to reach the central Irminger Basin is more like 2 years (Fig. 12). This implies a mean advective velocity of 1–2 cm/s, which is consistent with the mean velocities in the interior of the subpolar gyre. A possible explanation for this discrepancy is that local dense water formation might be occurring in the western Irminger Sea. This is addressed in Pickart et al. (2003). The estimate of Sy et al. for LSW to reach the Newfoundland basin via the DWBC (order 1 year) is consistent with our model findings.

5. Summary and discussion

Recently collected data have shown the presence of a series of recirculations and regions of high eddy kinetic energy in the northern subpolar gyre and, particularly, in the Labrador Sea. In this study we have investigated the role that these

features play in the spreading of LSW, a water mass formed by deep convection in the Labrador basin and found throughout the North Atlantic. The spreading of LSW is simulated using an advective-diffusive numerical model of the western North Atlantic subpolar gyre, based on a realistic flow field derived from PALACE floats. The initial location and area of LSW was taken from hydrographic data. The model was run in three different diffusive regimes, and it was found that the low to medium regimes were the most successful in reproducing the observations.

The model indicates that the initial spreading of LSW within the Labrador Sea is regulated by an interplay of advective and diffusive effects, and that these are of comparable magnitude. The subsequent export of tracer out of the basin, governed mostly by advective processes, occurs along two principal routes: a DWBC pathway and a Irminger Sea pathway. Export via the DWBC dominates, with up to 80% of LSW eventually exiting through this route, while only 20% of LSW makes it into the Irminger Sea. The recirculations in the interior of the Labrador Sea play an important role in determining the spreading pathways and their timing. In particular, the model revealed a new internal pathway, due to the westernmost recirculation in the Labrador Sea, which transports tracer eastward from the interior of the basin towards the West Greenland coast, where it is then mixed into the boundary current. A second recirculation, south of Greenland, is found to be important in feeding the Irminger Sea pathway. We have also investigated the impact of the high eddy kinetic energy region located west of Greenland; a feature which is evident in all surface and subsurface data collected in the region. Overall, we found that the impact of this maximum is limited, though it does contribute to a slightly faster flushing of the interior and spreading of tracer throughout the boundary current.

The DWBC and Irminger pathways resolved by our simulations are consistent with those proposed in a number of earlier studies. Because of the relatively poor resolution of the North Atlantic Current, however, our model was not able to shed light on the pathway into the eastern North Atlantic or on the possibility that LSW found in the Irminger basin may have arrived via the North Atlantic Current by way of the DWBC. Our estimates of the rate of spreading via the DWBC, and of a residence time of 4–5 years for the Labrador basin, are consistent with observations. We found that the time taken for LSW to reach the Irminger basin is on the order of a year and a half, at odds with recent estimates of only 6 months.

The model used in this study assumes that the presence of LSW does not modify the velocity field and that it can be treated as a passive tracer. While this is supported by the barotropic nature of the flow in the subpolar gyre, it is clearly a simplification and the interaction between LSW and the velocity field still needs to be addressed. A second potential weakness of this study involves the extent to which the mean velocity field observed by the floats between 1994 and 1998 is representative of other time periods. While we have shown that there exists qualitative support for this flow field in models and observations spanning different time periods, we acknowledge that there is considerable interannual variability in the subpolar gyre's circulation (and potentially in the interior flow field) that has not been addressed in this study.

Acknowledgements

FS would like to thank B. Owens, M. Spall and R. Davis for sharing their expertise, A. Bower for comments on an earlier version of the manuscript, and J. LaCasce, in particular, for many enlightening discussions. M. Spall kindly provided the model code. FS was supported by a grant from the Vetlesen Foundation through the Cooperative Institute for Climate and Ocean Research (CICOR).

References

Böning, C.W., 1988. Characteristics of particle dispersion in the North Atlantic: an alternative interpretation of SOFAR float results. Deep-Sea Research Part A 35, 1379–1385.

Clarke, R.A., Gascard, J.C., 1983. The formation of Labrador Sea Water. Part I: Large-Scale Processes. Journal of Physical Oceanography 13, 1764–1778.

Colin de Verdiere, A., 1983. Lagrangian eddy statistics from surface drifters in the eastern North Atlantic. Journal of Marine Research 41, 375–398.

Cuny, J., Rhines, P., Niiler, P., Bacon, S., 2002. Labrador Sea Boundary Currents and the fate of Irminger Water. Journal of Physical Oceanography 32, 627–647.

Curry, R.G., McCartney, M.S., 2001. Ocean gyre circulation changes associated with the North Atlantic Oscillation. Journal of Physical Oceanography 31, 3374–3400.

Curry, R.G., McCartney, M.S., Joyce, T.M., 1998. Oceanic transport of subpolar climate signals to mid-depth subtropical waters. Nature 391, 575–577.

Davis, R.E., 1987. Modeling eddy transport of passive tracers. Journal of Marine Research 45, 635–666.

Davis, R.E., 1991. Observing the general circulation with floats. Deep-Sea Research Part A. 38, S531–S571.

Davis, R.E., 1998. Preliminary results from directly measuring middepth circulation in the tropical and South Pacific. Journal of Geophysical Research 103, 24, 619–24,639.

Dickson, R., Lazier, J., Meincke, J., Rhines, P., Swift, J., 1996. Long-term coordinated changes in the convective activity of the North Atlantic. Progress in Oceanography 38, 241–295.

Fischer, J., Schott, F., 2002. Labrador Sea Water tracked by profiling floats—from the boundary current into the open North Atlantic. Journal of Physical Oceanography 32, 573–584.

Freeland, H.J., Rhines, P., Rossby, H.T., 1975. Statistical observations of trajectories of neutrally buoyant floats in the North Atlantic. Journal of Marine Research 33, 383–404.

Gascard, J.C., 1978. Mediterranean deep water formation. Baroclinic Instability and oceanic eddies. Oceanologica Acta 1, 315–330.

Gascard, J.C., Clarke, R.A., 1983. The formation of Labrador Sea Water. Part II: mesoscale and smaller-scale processes. Journal of Physical Oceanography 13, 1779–1797.

Hermann, A., Owens, B., 1993. Energetics of gravitational adjustment for mesoscale chimneys. Journal of Physical Oceanography 23, 346–371.

Holland, W.R., Chow, J.C., Bryan, F.O., 1998. Application of a third-order upwind scheme in the NCAR Ocean Model. Journal of Climate 11, 1487–1493.

Jakobsen, P.K., Ribergaard, M.H., Quadfasel, D., Schmith, T. The near surface circulation in the Northern North Atlantic as inferred from Lagrangian drifters: variability from the mesoscale to interannual. Journal of Geophysical Research, in press.

Käse, R.H., Biastoch, A., Stammer, D.B., 2001. On the mid-depth circulation in the Labrador and Irminger Seas. Geophysical Research Letters 28, 3433–3436.

Khatiwala, S., Schlosser, P., Visbeck, M., 2002. Rates and mechanisms of water mass transformation in the Labrador Sea as inferred from tracer observations. Journal of Physical Oceanography 32, 666–686.

Krauss, W., Böning, C.W., 1987. Lagrangian properties of eddy fields in the northern Atlantic as deduced from satellite-tracked buoys. Journal of Marine Research 45, 259–291.

Lab Sea Group, 1998. The Labrador Sea Deep Convection Experiment. Bulletin of the American Meteorological Society 79, 2033–2058.

LaCasce, J., Bower, A., 2000. Relative dispersion in the subsurface North Atlantic. Journal of Marine Research 58, 863–894.

Lavender, K., 2001. The general circulation and open-ocean deep convection in the Labrador Sea: a study using subsurface floats. Ph.D. Thesis, University of California, San Diego, p. 131.

Lavender, K., Davis, R.E., Owens, W.B., 2000. Mid-depth recirculation observed in the interior Labrador and Irminger Seas by direct velocity measurements. Nature 407, 66–99.

Lazier, J.R.N., 1973. The renewal of Labrador Sea Water. Deep-Sea Research 20, 341–353.

Lazier, J.R.N., 1995. The salinity decrease in the Labrador Sea over the past thirty years. Natural climate variability on decade-to-century time scales. National Research Council, Washington, DC, pp. 295–302.

Lilly, J.M., Rhines, P.B., 2002. Coherent eddies in the Labrador Sea observed from a mooring. Journal of Physical Oceanography 32, 585–598.

Lilly, J.M., Rhines, P.B., Visbeck, M., Davis, R., Lazier, J.R.N., Schott, F., Farmer, D., 1999. Observing deep convection in the Labrador Sea during winter 1994–1995. Journal of Physical Oceanography 29, 2065–2098.

Lilly, J.M., Rhines, P.B., Schott, F., Lazier, J.R.N., Send, U., Käse, R., Mertens, C., D'Asaro, E. Observations of the Labrador Sea eddy field. Progress in Oceanography, accepted for publication.

Marshall, J., Schott, F., 1998. Open-Ocean Convection: observations, theory and models, Vol. 52. Center for Global Change Science, Massachusetts Institute of Technology.

Maxworthy, T., Narimousa, S., 1994. Unsteady, turbulent convection into a homogeneous, rotating fluid, with oceanographic applications. Journal of Physical Oceanography 24, 865–887.

Molinari, R.L., Fine, R.A., Wilson, W.D., Curry, R.G., Abell, J., McCartney, M.S., 1998. The arrival of recently formed Labrador Sea water in the deep western boundary current at 26.5°N. Geophysical Research Letters 25, 2249–2252.

Owens, W.B., 1991. A statistical description of the mean circulation and eddy variability in the northwestern North Atlantic using SOFAR floats. Progress in Oceanography 28, 257–303.

Pickart, R.S., Spall, M.A., Lazier, J.R., 1997. Mid-depth ventilation in the western boundary current system of the sub-polar gyre. Deep-Sea Research I 44, 1025–1054.

Pickart, R.S., Torres, D.J., Clarke, R.A., 2002. Hydrography of the Labrador Sea During Convection. Journal of Physical Oceanography 32, 428–457.

Pickart, R.S., Straneo, F., Moore, G.W.K., 2003. Is Labrador Sea Water formed in the Irminger Basin? Deep-Sea Research I 50, 23–52.

Prater, M., 2002. Eddies in the Labrador Sea as observed by profiling RAFOS floats and remote sensing. Journal of Physical Oceanography 32, 411–427.

Rhein, M., Fischer, J., Smethie, W.M., Smythe-Wright, D., Weiss, R.F., Mertens, C., Min, D.H., Fleischmann, U., Putzka, A., 2002. Labrador Sea Water: pathways, CFC-inventory and formation rates. Journal of Physical Oceanography 32, 648–665.

Schäfer, H., Krauss, W., 1995. Eddy statistics in the South Atlantic as derived from drifter drogued at 100 m. Journal of Marine Research 53, 403–431.

Smith, R.D., Maltrud, M.E., Bryan, F.O., Hecht, M.W., 2000. Numerical simulation of the North Atlantic Ocean at $1/10^{\circ}$. Journal of Physical Oceanography 30, 1532–1561.

Spall, M., Pickart, R.S. Wind-driven recirculations and exchange in the Irminger and Labrador Seas. Journal of Physical Oceanography, in press.

Straneo, F., Kawase, M., 1999. Comparisons of localized convection due to localized forcing and to preconditioning. Journal of Physical Oceanography 29, 55–68.

Sy, A., Rhein, M., Lazier, J.R.N., Koltermann, K.P., Meincke, J., Outzka, A., Bersch, M., 1997. Surprisingly rapid spreading of newly formed intermediate waters across the North Atlantic Ocean. Nature 386, 675–679.

Talley, L.D., McCartney, M.S., 1982. Distribution and circulation of Labrador Sea Water. Journal of Physical Oceanography 12, 1189–1205.

Taylor, G.I., 1921. Diffusion by continuous movements. Proceedings of the London Mathematical Society 20, 196–212.

Zhang, H.-M., Prater, M.D., Rossby, T., 2001. Isopycnal Lagrangian Statistics from the North Atlantic Current RAFOS float observations. Journal of Geophysical Research 106, 13,817–13,836.